Journal of Marine Systems 215 (2021) 103501

Contents lists available at ScienceDirect

Journal of Marine Systems

journal homepage: www.elsevier.com/locate/jmarsys

Phytoplankton community structure in a contrasting physico-chemical regime along the eastern Arabian Sea during the winter monsoon

Anil Kumar Vijayan [a,*], B. Bikram Reddy [a,b], V. Sudheesh [a], Prachi Hemant Marathe [a,b], Vishnu N. Nampoothiri [a], N.V. Harikrishnachari [a], P. Kavya [c], G.V.M. Gupta [a], M. V. Ramanamurthy [a]

[a] Centre for Marine Living Resources and Ecology (CMLRE), Ministry of Earth Sciences, Cochin, India
[b] School of Ocean Sciences and Technology, Kerala University of Fisheries and Ocean Studies (KUFOS), Cochin, India
[c] Cochin University of Science and Technology, Cochin, India

ARTICLE INFO

Keywords:
Phytoplankton pigments
Eastern Arabian Sea
Winter convection
CHEMTAX

ABSTRACT

The paper describes the community composition of phytoplankton in the eastern Arabian Sea (EAS) during winter monsoon (WM, January–February 2018), encompassing the entire eastern part of the Arabian Sea basin (~6–22°N and 77–67°E) with high-resolution sampling (7 transects, 56 sites), from coastal to offshore regions. The phytoplankton pigment concentrations estimated by high-performance liquid chromatography were interpreted using 'CHEMTAX' (Mackey et al., 1996) to determine relative abundance and contribution of phytoplankton functional groups at the class level. A distinct spatial heterogeneity was observed in the distribution of phytoplankton groups in the coastal and offshore regions of the northern as well as southern part of the EAS. The basin-scale column integrated chlorophyll *a* (Chl *a*) concentration in the upper 100 m was higher (16–118 mg m^{-2}) in the northeastern Arabian Sea (NEAS) as against 9–79 mg m^{-2} in the southeastern Arabian Sea (SEAS). The chromatographic analysis revealed the dominance of diatoms in the coastal waters of the EAS basin. A closer evaluation of the hydrodynamics and nutrient chemistry of the offshore regions revealed that entrainment of subhalocline nutrients into the sunlit water column through convective mixing supported the dominant cyanobacterial population in the NEAS. In the warm oligotrophic waters of the SEAS, the substantially high NH_4^+ concentration indicates that the dominant prochlorophytes were sustained by the regenerated production. The dominance of large phytoplankton like diatoms indicates a herbivorous control in the food chain in coastal waters of the EAS. Offshore waters are characterised by large proportions of pico-nano plankton along with considerable micro phytoplankton, which suggests a mixotrophic ecosystem. The statistical analysis showed that the silicate (Si/N ratio) concentration played a major role in controlling the diatom abundance in the coastal areas of the north (south) EAS while temperature and salinity together with nutrients structured the phytoplankton assemblage in the offshore waters during WM.

1. Introduction

The unique nature of the monsoon system in the Arabian Sea (AS) creates two distinctly elevated high productive periods, viz. winter monsoon (WM) and summer monsoon (SM) (Wiggert et al., 2005). The convective mixing during WM and upwelling during SM makes the AS one of the most biologically productive regions in the world (Banse, 1987). During the WM, the cool and dry north-easterly winds propagate across the AS (Wiggert et al., 2002) leading to convective mixing which results in enhanced productivity in the northeastern Arabian Sea (NEAS), but not in the southeastern Arabian Sea (SEAS) (Madhupratap et al., 1996, 2001). During the SM, strong upwelling causes nutrient enrichment in the surface layers leading to high primary production in the SEAS (Wiggert et al., 2005; Gupta et al., 2016). On the other hand, during WM, a highly oligotrophic and stratified condition prevails over the SEAS, leading to a subsurface chlorophyll maxima (SCM) in the SEAS (Gupta et al., 2016). Moreover, the formation of high-saline waters over the NEAS and intrusion of the Bay of Bengal (BoB) waters into the SEAS creates a strong salinity gradient across the EAS basin during WM (Prasannakumar et al., 2004). These varying physical and

* Corresponding author.
E-mail address: anilkumarv@cmlre.gov.in (A.K. Vijayan).

https://doi.org/10.1016/j.jmarsys.2020.103501
Received 26 July 2020; Received in revised form 11 December 2020; Accepted 11 December 2020
Available online 20 December 2020

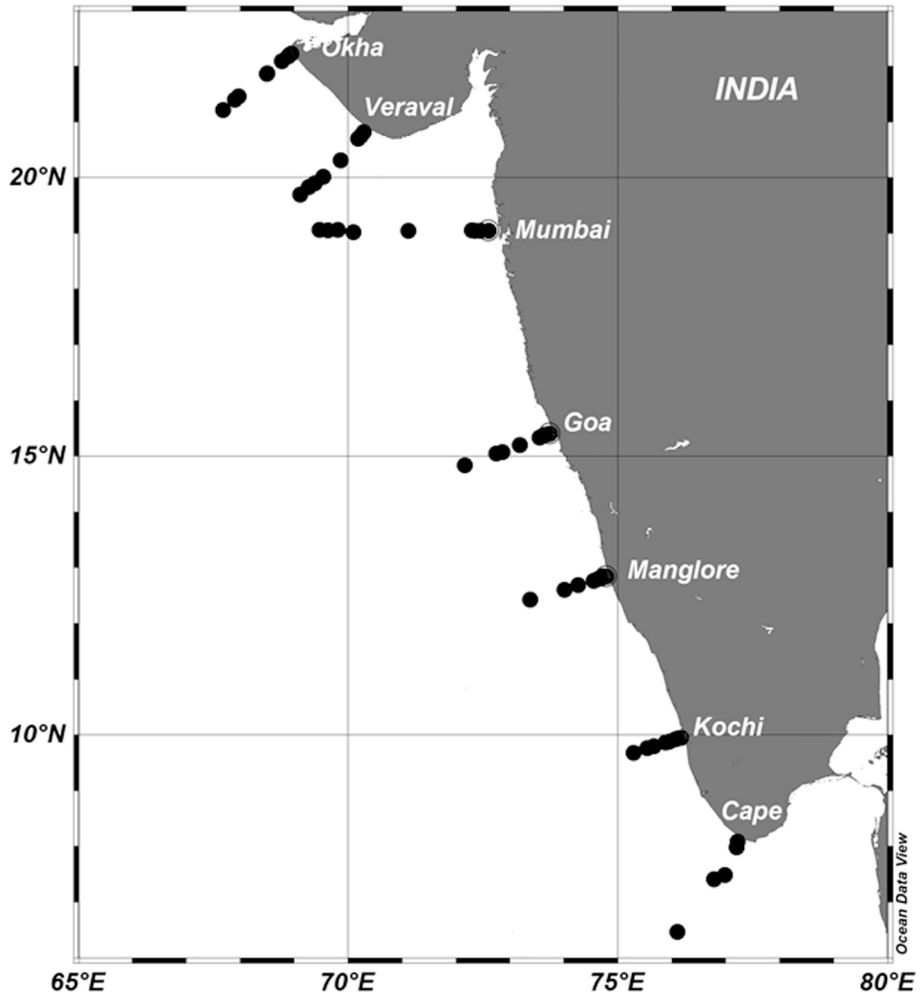

Fig. 1. Sampling locations along the eastern Arabian Sea. The transect up to 15°N (Cape, Kochi, Mangalore, and Goa) are defined as southeastern Arabian Sea (SEAS) and the other three northern transects (Mumbai, Veraval, and Okha) as northeastern Arabian Sea (NEAS). The stations from 10 to 50 m depth stations are grouped as coastal stations and those beyond up to 2000 m as offshore stations.

biogeochemical conditions give rise to basin-scale changes in plankton assemblages in both time and space. The phytoplankton community composition determines food web dynamics and influences the various biogeochemical processes of the ecosystem (Garrison et al., 2000).

In the past, many studies have been conducted in the EAS addressing the ecosystem level changes and seasonal cycles of phytoplankton (e.g., Qasim, 1977; Radhakrishna et al., 1978; Banse, 1987; Goes et al., 1992; Banse and English, 1993; Bhattathiri et al., 1996; Roy et al., 2006; Gomes et al., 2008). Although many of these studies had large spatial coverage, the sampling resolution was limited. Most of these studies were carried out either in coastal waters (Chacko, 1942; John and Menon, 1942; Subrahmanyan and Sarma, 1961, 1967; Devassy et al., 1978, 1979; Devassy and Goes, 1988; Sawant and Madhupratap, 1996) or were limited to open ocean waters alone (JGOFS-US, JGOFS-INDIA). Some studies also covered the shelf and slope regions but with minimal sampling (Parab et al., 2006). In the past decade, studies related to phytoplankton dynamics during the WM mostly focussed on winter bloom dynamics or the phytoplankton community structure associated with physical features like eddies or fronts in the open ocean regions of NEAS (Roy et al., 2015; Baliarsingh et al., 2018; Bemal et al., 2018; Lotliker et al., 2018; Sarma et al., 2018 and references therein). Similarly, biological studies in the SEAS region either concentrated on SM upwelling (e.g., Thomas et al., 2013; Padmakumar et al., 2010; Ahmed et al., 2016) or were restricted to coastal areas (Krishnankutty et al., 2019; Minu et al., 2014; Rai and Rajashekhar, 2014).

The chemotaxonomic studies on phytoplankton pigment signatures are valuable in determining the composition and abundance of phytoplankton populations (Wright et al., 1991; Jeffrey et al., 1997; Bidigare and Charles, 2002). Biomarker pigment signatures can reveal class-specific taxonomic composition (Wright et al., 1991; Jeffrey and Vesk, 1997), physiological status (Jeffrey and Wright, 1997), and food web structure (Legendre and Rassoulzadegan, 1995) under a variety of environmental conditions (Vidussi et al., 2001; Roy and Anil, 2015; Roy et al., 2015; Chndrasekhararao et al., 2018). Besides this, the diagnostic pigment indices and pigment ratios are used to determine phototroph groups (pico, nano, and micro phytoplankton). There have been many phytoplankton pigment-based studies in the western and central Arabian Sea linking the monsoon seasonal cycles and phytoplankton community (Latasa and Bidigare, 1998; Barlow et al., 1999; Goericke, 2002; Brown et al., 2002). The knowledge on the photosynthetic pigments in the EAS mainly came from the studies of Parab et al. (2006), Roy et al. (2006, 2015), Roy (2010), Roy and Anil (2015), Ahmed et al. (2016), Bemal et al. (2018) and Chndrasekhararao et al. (2018). These studies revealed that the abundance and composition of the phytoplankton community are strongly influenced by the change in environmental conditions associated with ecosystem dynamics.

Though there are several studies on the physical dynamics of the EAS, most of the biogeochemical and biological studies are confined to a region, i.e., either NEAS or SEAS. A basin-wide understanding is hitherto lacking, which is, in turn, found to obscure the factors supporting

Table 1
The pigment symbol, names, formulae and their chemotaxonomic relation used in this study (Gibb et al., 2001; Jeffrey et al., 1997)

Pigment	Abbreviation	Designation of phytoplankton groups
Chlorophyll a	Chl *a*	Total algal biomass (including cyanobacteria)
Chlorophyll b	Chl *b*	Chlorophytes, prasinophytes
Chlorophyll c_1c_2	Chl C2	Diatoms, prymnesiophytes, cryophytes, dinoflagellates
Chlorophyll c3	Chl C3	Prymnesiophytes, crysophytes
Alloxanthin	Allo	Cryptophytes
19'butanoyloxyfucoxanthin	19'BF	Chrysophytes, prymnesiophytes
Divinyl chlorophyll a	DVChl a	Prochlorophytes
Fucoxanthin	Fuco	Diatoms, prymnesiophytes, chrysophytes
19'hexanoyloxyfucoxanthin	19'HF	prymnesiophytes
Lutein	Lut	Chlorophytes, prasinophytes
Peridinin	Peri	Dinoflagellates
Prasinoxanthin	Pras	Prasinophytes
Zeaxanthin	Zea	Cyanobacteria, Prochlorophytes
Violaxanthin	Viola	Chlorophytes, Prasinophytes
Neoxanthin	Neo	Green algae
Diadinoxanthin	Diad	Diatoms, Dinoflagellates
Dinoxanthin	Dino	Dinoflagellates
Diatoxanthin	Diat	
Antheraxanthin	Anthera	
Phaeophorbide	Phaeo	Chlorophyll degradation products

biological resources in the eastern Arabian Sea. The present study, therefore, is a comprehensive investigation of the phytoplankton community along the EAS during WM, with both an extensive spatial scale and high-resolution sampling, focussed on (i) difference in the distribution of phytoplankton community under a warm, oligotrophic, and cold, nutrient-rich condition, (ii) phytoplankton community composition at the subsurface chlorophyll maxima (SCM).

2. Materials and methods

The study was carried out as part of the project "Marine Ecosystem Dynamics of eastern Arabian Sea (MEDAS)". It is the first study of its kind to encompass the entire eastern part of the Arabian Sea basin (between ~6–22°N and 77–67°E) with high-resolution sampling from coastal to offshore regions (Fig. 1). Observations were conducted onboard FORV *Sagar Sampada* covering seven coast-offshore transects (Cape, Kochi, Mangalore, Goa, Mumbai, Veraval, and Okha) along the EAS during the winter monsoon (January–February) of 2018. At each transect, 8–10 stations were covered with depths ranging between 10 and 2000 m. The EAS was divided into two regions: north EAS (NEAS) and south EAS (SEAS). The transects up to 15°N (Cape, Kochi, Mangalore, and Goa) are grouped under the SEAS, and the other three northern transects (Mumbai, Veraval, and Okha) are defined as NEAS. For the convenience of discussion, the 10–50 m depth stations are grouped as coastal stations and those beyond (up to 2000 m) as offshore stations.

Continuous profiles of salinity and temperature were recorded using a Conductivity-Temperature-Depth (CTD) profiler (SBE 11 Plus, Sea-Bird, USA). The dissolved oxygen (DO) profiles were recorded using an SBE 43 sensor attached to the CTD rosette. All the sensors have been factory calibrated before the commencement of the field campaign. The temperature and salinity sensors have an analytical precision of ±0.0005 °C and ±0.001 (SBE 9plus) and the DO sensor can perform an accuracy of ±2% of saturation. The sensors were cleaned frequently using 1% Tripton-100 to maintain its performance.

Water samples were collected from standard depths using 12 L Niskin samplers attached to CTD Rosette. Sub-samples for nutrients were filtered through GF/F filter, and the filtrate was collected in HDPE bottles (60 and 100 ml) and poisoned with saturated $HgCl_2$. Nutrients (nitrite, phosphate and silicate) were analysed using an autoanalyser (SKALAR SAN++) following Grasshoff et al. (1999). Nitrate was analysed using the autoanalyser but following the method of García-Robledo et al. (2014). Ammonium was measured spectrophotometrically (Thermo Evolution 201) immediately after collection, following standard procedures (Grasshoff et al., 1999). The analytical precisions, expressed as standard deviation based on replicate analyses, were ±0.005, 0.027, 0.009, 0.037, and 0.1 μM for NO_2-, NO_3-, PO_4^{3-}, SiO_4^{2-} and NH_4^+, respectively.

Sub-samples (0.5–2 L) for phytoplankton pigments were filtered onboard through Whatman GF/F filters (0.7 μm, 25 mm) under dark conditions and stored at −80 °C. The filters were extracted in 3 ml of 100% methanol using ultrasonicator (QSONICA Q55), filtered using Teflon syringe PTFE membrane (PALL ValuePrep, 0.22 μm, 25 mm) and the pigments were analysed using HPLC (Shimadzu Prominence) following Van Heukelem (2002) as described in Roy et al. (2015). The entire analysis from filtration till sample injection was carried out in dim light and at low temperature to minimise degradation of pigments. The eluting pigments were detected at 450 and 665 nm (Soret and Qy bands) by the diode array detector. Identification and quantification of 20 different phytoplankton pigments (Table 1) were performed by comparing the retention time and visible spectra with standards obtained from DHI Inc., Denmark. Limits of detection were of the order of 0.001 μg l^{-1}.

To know the proportion of each community such as diatoms, nanoflagellates, and prokaryotes, the diagnostic pigment indices (DP, in μg l^{-1}) were calculated using seven pigments *viz.* fucoxanthin, peridinin, 19'butanoyloxyfucoxanthin, 19'hexanoyloxyfucoxanthin, alloxanthin, chlorophyll b and zeaxanthin (Barlow et al., 2007) as follows:

$$\text{FlagDP} = (\text{Allo} + 19'\text{HF} + 19'\text{BF} + \text{Chl b})/\text{DP}$$

$$\text{ProkDP} = \text{Zea}/\text{DP}$$

$$\text{Diatom}_{\text{DP}} = \text{Fuco}/\text{DP}$$

In the above equation, DP is the sum of the above mentioned 7 pigments.

The fractions of the Chl *a* concentration associated with each of the three phytoplankton classes (f_{micro}, f_{nano} and f_{pico}) were then derived using the weighted sum of all the diagnostic pigment concentrations, ΣDPw, expressed (Uitz et al., 2006) as follows

Table 2
Marker pigments to Chl *a* ratio of the eight taxonomic groups. Input ratios were obtained from Schlüter et al. (2000) and Gibb et al. (2001).

	Peri	19'BF	Fuco	19'HF	Allo	Pras	Viola	DVChl *a*	Lut	Zea	Chl *b*	Chl *a*
(a) *Input matrix*	0	0	0	0	0	0.315	0.062	0	0.009	0	0.238	1
Prasinophytes	1.063	0	0	0	0	0	0	0	0	0	0	1
Dinoflagellates	0	0	0	0	0	0	0	0.186	0	0	0	1
prochlorophytes	0	0	0	1.706	0	0	0	0	0	0	0	1
Haptophytes	0	0	0	0	0.530	0	0	0	0	0	0	1
Cryptophytes	0	0	0	0	0	0	0.055	0	0.203	0.009	0.263	1
Chlorophytes	0	0	0	0	0	0	0	0	0	0.348	0	1
Cyanobacteria	0	0	0.432	0	0	0	0	0	0	0	0	1
Diatoms	0	0	0	0	0	0.315	0.062	0	0.009	0	0.238	1

Table 3
Estimated output ratios based on CHEMTAX analysis.

	Peri	19'BF	Fuco	19'HF	Allo	Pras	Viola	DVChl *a*	Lut	Zea	Chl *b*	Chl *a*
(b) *Output matrix*	0	0	0	0	0	0.194	0.038	0	0.005	0	0.147	0.616
Prasinophytes	0.515	0	0	0	0	0	0	0	0	0	0	0.485
Dinoflagellates	0	0	0	0	0	0	0	0.364	0	0	0	0.636
Prochlorophytes	0	0	0	0.630	0	0	0	0	0	0	0	0.370
Haptophytes	0	0	0	0	0.346	0	0	0	0	0	0	0.654
Cryptophytes	0	0	0	0	0	0	0.032	0	0.133	0.006	0.173	0.656
Chlorophytes	0	0	0	0	0	0	0	0	0	0.258	0	0.742
Cyanobacteria	0	0	0.296	0	0	0	0	0	0	0	0	0.704
Diatoms	0	0	0	0	0	0.194	0.038	0	0.005	0	0.147	0.616

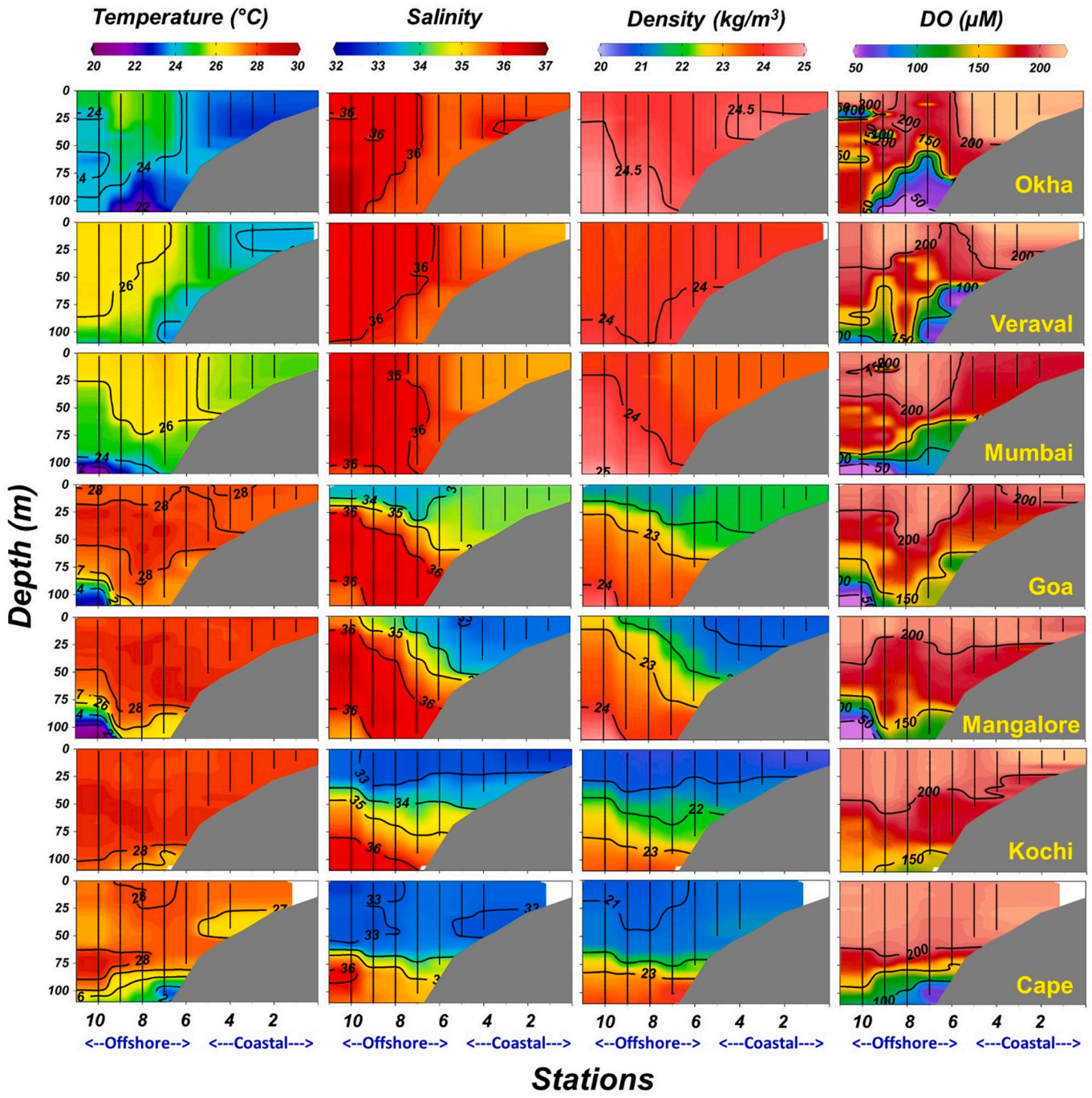

Fig. 2. Spatial variation in (a) temperature (b) salinity (c) density (d) dissolved oxygen along the EAS during WM 2018.

$$\sum \text{DPw} = 1.41[\text{Fuco}] + 1.41[\text{Peri}] + 1.27[19'\text{HF}] + 0.35[19'\text{BF}] + 0.6[\text{Allo}] + 1.01[\text{TChl } b] + 0.86[\text{Zea}]$$

$$f\text{micro} = (1.41[\text{Fuco}] + 1.41[\text{Peri}]) / \sum \text{DPw}$$

$$f\text{nano} = (1.27[19'\text{HF}] + 0.35[19'\text{BF}] + 0.60[\text{Allo}]) / \sum \text{DPw}$$

$$f\text{pico} = (1.01[\text{Chl } b] + 0.86[\text{Zea}]) / \sum \text{DPw}$$

The total Chl *a* (TChl *a*) biomass of various phytoplankton groups were calculated from the biomarker pigment concentration by factor analysis and steepest-descent algorithm to find the best fit on to an initial pigment ratio matrix using the CHEMTAX software (Mackey et al., 1996; Wright et al., 2009, 2010) following the procedure detailed in Mackey et al. (1996). An initial pigment ratio to Chl *a* for each indicator pigment was obtained from Gibb et al. (2001) and Schlüter et al. (2000). The contribution of diatoms, cyanobacteria, prochlorophytes, haptophytes, chlorophytes, prasinophytes, cryptophytes, and dinoflagellates to TChl *a* was calculated using CHEMTAX. The pigments used were peridinin, 19'butanoyloxyfucoxanthin, fucoxanthin, 19'hexanoyloxyfucoxanthin, alloxanthin, prasinoxanthin, violaxanthin, divinyl chlorophyll *a*, lutein, zeaxanthin, Chl *b*, Chl *a*. To maintain the sensitivity of the input values, CHEMTAX input ratios were optimised following Wright et al. (2009), and the output with smallest residual was chosen as detailed in Roy et al. (2015). Table 2 lists the pigment ratios used in the calculation and Table 3 shows the estimated output ratio derived by CHEMTAX program, which assumes that the relative amount of each marker pigment to TChl *a* is constant within a particular group of phytoplankton.

The influence of different environmental parameters (temperature, salinity, dissolved oxygen, inorganic nutrients, and their ratio) on the distribution of different phytoplankton size fractions (f_{micro}, f_{nano} and f_{pico}) were analysed through a principal component analysis (PCA) in PRIMER® ver. 6 (Warwick and Clarke, 2006). The statistical analysis, like PCA and PERMANOVA, was done after log-transformation and normalisation of the data.

3. Results

3.1. Hydrographic variations

The hydrographic conditions separated the EAS into two distinct regions during the study period; surface waters were cold (23.3–26.9 °C), high-saline (35.2–36.4) in the NEAS; while a warmer (27.4–28.4 °C), low-saline (32.6–35.5) condition prevailed in the SEAS (Fig. 2a, b). The prevalence of cold high saline waters in the NEAS shows the signatures of convective mixing that were found prominent at the northernmost transect (Okha) and the signals were weaker towards the southern part of NEAS. The SST was ~3–4 °C warmer in the SEAS than the NEAS. The warm (>28 °C), low-saline (<34.5) layer in the offshore waters (upper 60 m) of the southern SEAS (Cape, ~7°N) reveals the intrusion of BoB waters, which thinned towards the north and was restricted to the upper ~10 m of the water column at ~15°N (Goa). The coastal waters were well-mixed throughout the EAS with distinct characteristics in the NEAS and SEAS. While the coastal waters of the SEAS (up to ~15°N) were influenced by BoB waters (<34.5), the Arabian Sea High Saline Water mass (>35.3) occupied coastal waters of the NEAS (Fig. 2b). The occurrence of a thermal inversion with a magnitude of 0.2–0.3 was noticed from Cape to Goa between 25 and 75 m depth. Mixed layer depth (MLD) in the offshore waters varied from 8 to 64 m and 18 to 99 m respectively, in the SEAS and NEAS.

3.2. Distribution of inorganic nutrients

The average nutrient concentrations (NO_3^-, PO_4^{3-}, SiO_4^{2-}) in the water column in the NEAS coastal waters were significantly higher compared to similar regions of the SEAS, except NH_4^+ which showed a reverse trend (Table 4). The N/P ratio was relatively higher in the NEAS coastal water (6.7±3.8) than the SEAS (4.0±2.3). The higher Si/N and Si/P ratios were recorded in the SEAS (4.4±3.4 and 13.0±5.5) as against the similar regions of the NEAS (1.8±0.9 and 9.7±4.6).

In the offshore waters, the average nutrient concentrations in the MLD were lower in the SEAS compared to the NEAS (Table 4). The N/P and Si/N ratios were comparable in both SEAS (5.8±2.1 and 1.6±0.9) and the NEAS (4.9±2.3 and 1.6±0.8) while Si/P recorded relatively higher in the SEAS (8.7±5.0) than the NEAS (6.4±1.6). Below the MLD and up to 100 m, the N/P ratios were relatively higher in the NEAS than the SEAS offshore waters (9.9±2.6 and 7.5±3.3), but both were significantly lower than the Redfield ratio (16:1). Relatively lower Si/N and Si/P ratios were recorded below the mixed layer in the offshore waters of the NEAS (0.7±0.1 and 6.9±1.9) compared to the SEAS (1.2±1.2 and 7.5±3.9).

3.3. Spatial distribution of Chl a and contribution of accessory pigments in the EAS

The coastal waters of the EAS were characterised by high Chl *a* (>1 μg l^{-1}) than the offshore waters with maximum concentration in the NEAS which waned towards the south. Though Chl *a* values generally remained low (≤0.8 μg l^{-1}) in the offshore regions, the highest biomass of 5.2 μg l^{-1} was also recorded at the NEAS (2000 m depth station, off Okha) (Fig. 4a). The surface Chl *a* showed higher values (2.21±1.25 μg l^{-1} in coastal and 1.08±1.26 μg l^{-1} in offshore waters) in NEAS compared to SEAS (0.84±0.95 μg l^{-1} in coastal and 0.09±0.02 μg l^{-1} in offshore waters). The basin-scale depth-integrated (up to 100 m) Chl *a* concentration (∑Chl *a*) was also higher in the NEAS (16–118 mg m^{-2}) as against 9–79 mg m^{-2} in the SEAS.

The chromatographic analysis recorded a suite of marker pigments, indicating the occurrence of various algal groups, viz. diatoms, prymnesiophytes, prochlorophytes, cyanobacteria, etc. Diatoms (Fucoxanthin), Prochlorophytes (Divinyl Chlorophyll *a, b*), Cyanophyceae (Zeaxanthin), Prymnesiophytes (19' hexanoyloxyfucoxanthin), and Chlorophytes (Chl *b*) contributed to the major share of phytoplankton biomass (Refer Table 1).

3.3.1. Phytoplankton pigments in the NEAS

Fucoxanthin, a photosynthetic marker pigment for diatoms was the most dominant among accessory pigments in the coastal waters of the EAS (Fig. 4f) with higher values in the NEAS (0.68±0.53 μg l^{-1}). The second dominant pigment was Chl C2 (0.41±0.34 μg l^{-1}, Fig. 4c). The fucoxanthin: TChl *a* (0.17±0.11) and Chl C2: TChl *a* (0.19±0.05) ratios were high in the water column indicating the dominance of diatoms. Zeaxanthin was recorded in low concentration (0.19±0.05 μg l^{-1}). All other diagnostic pigments were recorded in trace or very low concentrations.

Table 4
Physico-chemical characteristics in the mixed layer waters of the EAS during WM 2018

Parameters	Offshore		Coastal	
	SEAS	NEAS	SEAS	NEAS
Temperature	28.0±0.3	26.0±0.8	28.0±0.3	24.7±1.1
Salinity	33.5±0.8	36.1±0.2	33.4±0.6	35.6±0.2
NO_3^-	0.2±0.3	1.7±2.6	0.2±0.2	5.7±5.9
NO_2^-	0.04±0.1	0.5±0.2	0.2±0.3	0.5±0.4
NH_4^+	1.3±0.5	0.9±0.4	1.1±0.4	0.6±0.1
PO_4^{3-}	0.3±0.1	0.5±0.2	0.4±0.2	0.9±0.3
SiO_4^{2-}	2.0±0.4	3.3±1.8	4.2±2.0	9.5±6.8
N/P	5.8±2.1	4.9±2.3	4.0±2.3	6.7±3.8
Si/N	1.6±0.9	1.6±0.8	4.4±3.4	1.8±0.9
Si/P	8.7±5.0	6.4±1.6	13.0±5.5	9.7±4.6

In the NEAS, the accessory pigments were higher in the surface waters, which gradually decreased with depth. The marker pigments for prymnesiophytes were recorded in higher concentration (up to 50 m depth) in the offshore regions of the NEAS (19'hexanoyloxyfucoxanthin: 0.41±0.004 μg l^{-1}; 19'butanoyloxyfucoxanthin: 0.06±0.05 μg l^{-1}; Chl C3: 0.14±0.09 μg l^{-1}) (Fig. 4.h, i, d). Elevated concentrations of zeaxanthin (≥0.1 μg l^{-1}) were observed in the ca. 30 m (Fig. 4g) while Chl *b* (≥0.05 μg l^{-1}) recorded up to ca. 50 m water column (Fig. 4b). Divinyl Chl *a* showed very low to below detectable levels in the NEAS (Fig. 4e). Fucoxanthin (0.08±0.06 μg l^{-1}) and Chl C2 (0.10±0.07 μg l^{-1}) were observed at significant levels in the NEAS offshore stations also. Peridinin was consistently a minor pigment and showed a maximum of 0.04 μg l^{-1} off Okha. The marker pigments neoxanthin, prasinoxanthin, violaxanthin, antheraxanthin, alloxanthin, lutein, etc. were recorded in very low or trace concentrations.

3.3.2. Phytoplankton pigments in the oligotrophic waters of the SEAS

Fucoxanthin was the dominant photosynthetic marker pigment (0.15±0.14 μg l^{-1}) in the coastal waters of SEAS (Fig. 4f). The Chl *b* (0.13±0.24 μg l^{-1}) and zeaxanthin (0.13±0.09 μg l^{-1}) were found to be subdominant accessory pigments in the coastal waters of SEAS (Fig. 4b, g). Chl *b* showed its peak values (≥1 μg l^{-1}) at surface layers (<10 m) in the inner shelf regions (up to 30 m station) off Goa. Concurrent strong signals of lutein (≥0.3 μg l^{-1}), neoxanthin (≥0.1 μg l^{-1}), violaxanthin (≥0.1 μg l^{-1}), and zeaxanthin (≥0.2 μg l^{-1}) were also recorded, which points towards the dominance of chlorophytes and cyanobacteria. Similarly, elevated concentrations of zeaxanthin (max. 0.2 μg l^{-1}) and DVChl *a* (max. 0.1 μg l^{-1}) along with low concentrations of Chl *b* (≤0.05 μg l^{-1}) were observed in the surface waters off Mangalore, suggesting a subdominant population of prochlorophytes. But the subsurface waters of this region showed diatom dominance, as revealed by high fucoxanthin (≥0.2 μg l^{-1}) which coincides with the SCM. The other diagnostic pigments were recorded in trace or very low concentrations in the coastal waters of the SEAS.

In the offshore waters of the SEAS, zeaxanthin, a photoprotective pigment, and biomarker for *Prochlorococcus*, *Synechococcus*, and present in cyanobacteria was abundant (~0.05 μg l^{-1}) in the upper 50 m. In the upper 20 m, the water column zeaxanthin concentration exceeded ≥0.15 μg l^{-1} with low total Chl *b* (which is inclusive of divinyl form) concentrations (≤0.05 μg l^{-1}). Between ca. 20 m to ca. 50 m, moderately high levels (~0.05 μg l^{-1}) of zeaxanthin was observed. Another interesting observation was the build-up of DVChl *a* (≥0.1 μg l^{-1}) which is an unequivocal marker pigment for prochlorophytes in the upper 50 m. The biomarker pigment 19'hexanoyloxyfucoxanthin was relatively low compared to the NEAS offshore (~0.05 μg l^{-1}). The co-occurrence of high concentration of the pigments 19'butanoyloxyfucoxanthin and Chl C3 (0.02±0.02 and 0.04±0.04 μg l^{-1}, respectively) indicate the abundance of prymnesiophytes in the subsurface layer which coincides with the SCM.

3.4. Characteristics of subsurface chlorophyll maxima (SCM)

The SCM was not observed in the NEAS offshore waters where Chl *a* was found well-distributed in the upper 50 m water column with a maximum observed in the surface layers (Fig. 4a). In the coastal waters, the SCM was located just above the bottom. The offshore waters of the SEAS are characterised by warm, oligotrophic surface layers where the SCM was observed at ca. 20–80 m (Fig. 4a). In coastal waters of the SEAS, the Chl *a* concentration of SCM variability was more (0.12–1.69 μg l^{-1}), while in the offshore waters the variability was marginal (0.3–0.8 μg l^{-1}). Fucoxanthin was the dominant pigment in the SCM of coastal waters (Fig. 4f). In the stratified offshore regions of the SEAS, the SCM was primarily constituted by DV Chl *a* (≥0.1 μg l^{-1}) followed by 19'hexanoyloxyfucoxanthin (≥0.05 μg l^{-1}), Chl C3 (≥0.05 μg l^{-1}), and Chl *b* (≥0.05 μg l^{-1}).

3.5. Spatial distribution of pigment indices and phytoplankton community structure

For a meaningful interpretation of pigment data, pigment indices were calculated. A good correlation (linear) was obtained between DP and Chl *a* (r^2 = 0.90, n = 260, p<0.001) which indicates the DP as a valid proxy for phytoplankton biomass. The basin-wide distributional pattern of pigment indices $Diat_{DP}$, $Flag_{DP}$, $Prok_{DP}$ revealed that large cells were abundant in the coastal regions while smaller cells flourished in the offshore waters of the EAS (Fig. 5). In the SEAS, the upper 30 m water column was dominated by prokaryotes ($Prok_{DP}$ >0.6) below which flagellate abundance ($Flag_{DP}$ >0.8) was observed. The CHEMTAX program was used to determine the contribution of 8 major taxonomic groups to the TChl *a*.

3.5.1. Phytoplankton community structure in the NEAS

The CHEMTAX program was used to determine the contribution of 8 major taxonomic groups to the TChl *a*. The analysis showed that diatoms were the major contributor to TChl *a* in the coastal waters of the NEAS (max. 3.92 μg l^{-1}) followed by cyanobacteria (max. 0.36 μg l^{-1}) (Fig. 6g, h). The NEAS offshore regions were dominated by cyanobacteria (max. 0.47 μg l^{-1}) and diatoms (max. 0.25 μg l^{-1}) followed by haptophytes (max. 0.20 μg l^{-1}) and prasinophytes (max 0.11 μg l^{-1}). All these groups were concentrated in the upper 75 m layer. The prochlorophytes were absent in the NEAS particularly north of 19°N (Fig. 6d).

3.5.2. Phytoplankton community structure in the SEAS

Diatoms were the dominant phytoplankton group in the SEAS coastal waters with the highest abundance near the bottom layers (max. 1.41 μg l^{-1}). The second dominant group was cyanobacteria (max. 0.88 μg l^{-1}) and their aggregation was mostly found in the surface layer. A spike in the abundance of chlorophytes was observed in the coastal waters off Goa (max. 4.31 μg l^{-1}) (Fig. 6f). The SEAS offshore regions were characterised by a dominance of prochlorophytes (max. 0.26 μg l^{-1}) and cyanobacteria (max. 0.15 μg l^{-1}), which were more prominent in the SCM layer. This region has also shown diatom abundance (0.06±0.06 μg l^{-1}), but with significantly less dominance compared to the similar regions of the NEAS. The haptophytes were a less significant group and were associated with SCM in the SEAS offshore region. The cryptophytes and dinoflagellates were consistently a minor group in the SEAS offshore and in the entire EAS respectively.

3.6. Statistical analysis

The difference in the influence of physico-chemical parameters on phytoplankton community structure between regions (NEAS and SEAS), was tested using PERMANOVA analysis and it was found to be statistically significant (pseudo-F= 28.23, p=0.001). In the PCA analysis, five principal components together explained 91.8% variance among the samples (Fig. 7). Out of these, PC 1 (Eigenvalues = 5.69) and PC 2 (Eigenvalues= 1.5a) together explained 72% variance in the data. The statistical analysis revealed a significant role of silicate in controlling the micro phytoplankton in the coastal areas of NEAS. At the same time, the Si/N ratio played a key role in the SEAS coastal waters. The physico-chemical factors like temperature, salinity, DIN, DIP, N/P ratios played a significant role in defining the pico-nano phytoplankton in the offshore waters.

4. Discussion

Phytoplankton responds rapidly to variations in ambient environmental conditions, which affects their distributional pattern, including the community structure (Chisholm, 1992). The difference in physico-chemical characteristics divided the EAS basin into two distinct ecosystems SEAS and NEAS during WM. While the SEAS was characterised by a warm, low-saline oligotrophic environment; a cold, high-saline,

nutrient-rich condition prevailed over the NEAS waters. This difference in physico-chemical condition significantly altered the phytoplankton distribution and its community structure over the EAS basin.

4.1. Influence of hydrographic features to the phytoplankton community in EAS

The distribution of phytoplankton communities and its variabilities are largely related to changes in environmental conditions (Barlow et al., 2002; Trees et al., 2000) including temperature (Bouman et al., 2003, 2005), irradiance, and vertical transport of nutrients from deeper water masses to surface layers (Legendre and Demers, 1984). During the WM, convective mixing is the major physical process that prevailed over the NEAS and was responsible for the nutrient entrainment to the surface layer. However, in the SEAS, strong stratification caused by the warmer surface water and low saline BoB water restricted the nutrient supply from the subsurface layer. This led to the formation of a SCM in the SEAS waters. While the persistence of SCM (~1.0 mg m^{-3}) was reported throughout the year in the EAS (Matondkar et al., 2006), the present study observed significant variability in SCM magnitude both zonally and meridionally. Chl *a* concentration of the SCM ranged from 0.12-1.69 μg l^{-1} in the coastal waters of the SEAS while in the offshore waters the values were 0.3-0.8 μg l^{-1}. The SCM closely followed the thermal inversion layer along the SEAS offshore waters.

The prochlorophytes which were recorded in higher abundance in the warmer (>27 °C), low saline waters (<33.5) of the SEAS offshore,

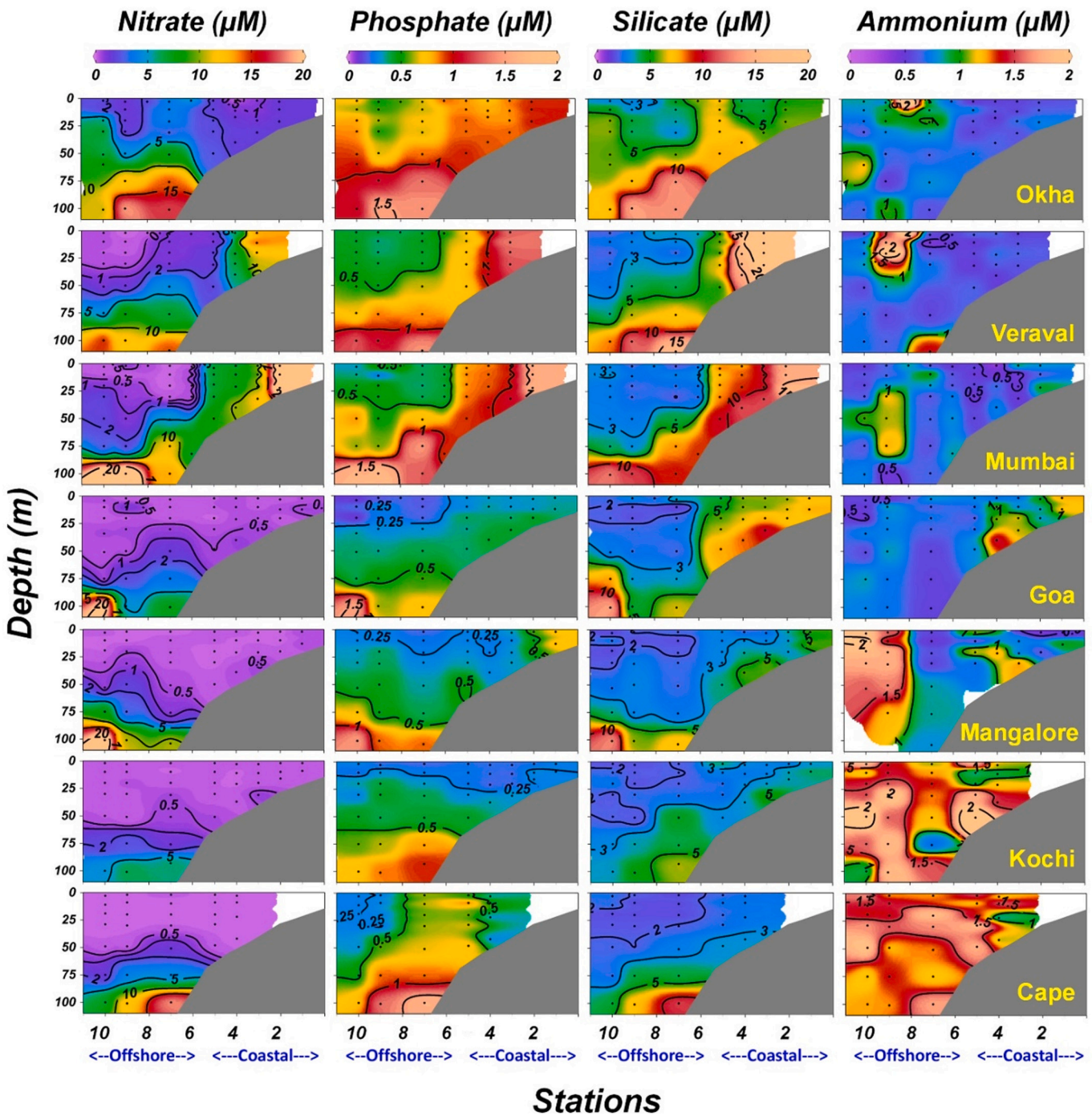

Fig. 3. Distribution of nutrients along the EAS during WM 2018.

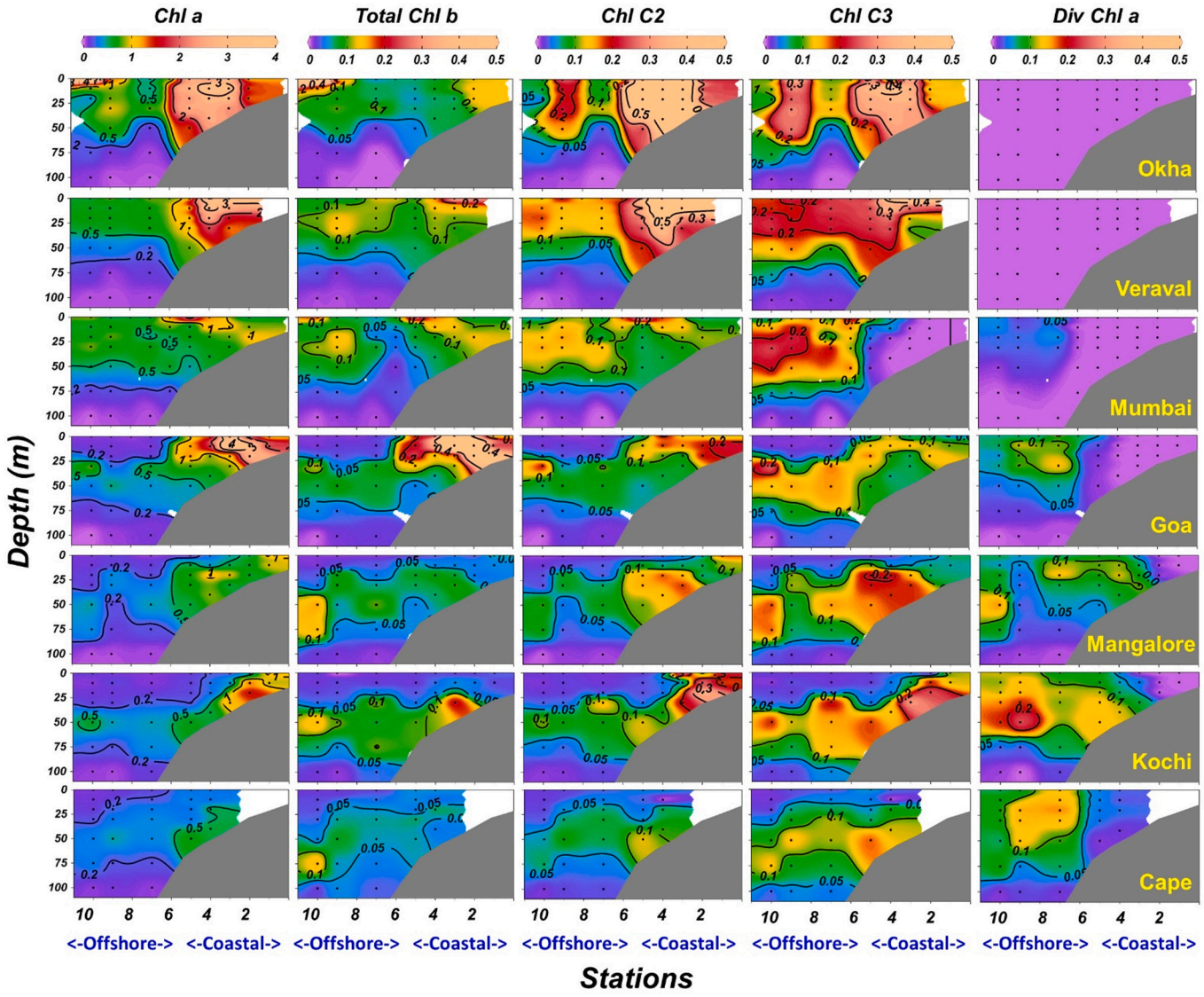

Fig. 4. Spatial distribution of (a) Chl *a* (b) Total Chl b (c) Chl C2 (d) Chl C3 (e) DVChl *a* along the EAS during WM 2018. Spatial distribution of (f) Fucoxanthin (g) Zeaxanthin (h) 19' hexanoyloxyfucoxanthin (i) 19' butanoyloxyfucoxanthinalong the EAS during WM 2018.

decreased gradually towards the north and were completely absent in colder (<25 °C), high saline (>36) waters. Previous studies in AS indicated that temperature (Shalapyonok et al., 2001; Chndrasekhararao et al., 2018) and irradiance, together with biogeochemical conditions (Roy and Anil, 2015) control the distribution of *Prochlorococcus* populations. Review of literature also reveals that the occurrence of *Prochlorococcus* cells are not restricted to offshore regions but that they are able to thrive in a wide range of salinity conditions (0.06–35). *Prochlorococcus* (like) cells are reported from estuaries (Mitbavkar et al., 2012), river plumes (Vaulot et al., 1990; Jochem, 2003) and atolls/lagoons (Charpy and Blanchot, 1996). However, the influence of salinity on the distribution of *Prochlorococcus* is not reported so far. The present study recorded a significant influence of salinity ($p<0.01$) on this group, suggesting that in addition to light, temperature and biogeochemical conditions, salinity is also a major factor in controlling the population of prochlorophytes in the AS. Along the coastal region of the EAS, diatom abundance was high. From the cooler waters of NEAS to the warmer SEAS waters, the diatoms showed a decreasing trend in their contribution to total phytoplankton pigment biomass. Though statistical analysis showed a significant negative (positive) correlation with temperature (salinity) (Pearson's test, $p<0.01$) on a basin scale, such significant relations were not observed within the SEAS or NEAS. This suggests that diatom abundance could have a bearing on the ambient nutrient conditions.

4.2. Phytoplankton community structure in contrasting biogeochemical regimes

Nutrients play a crucial role in regulating the productivity of the photic zone in the marine environment (Redfield, 1958). The proliferation of diatoms is generally associated with the nutrient status of the ecosystem. In our observation, their abundance was high in the nutrient-rich, waters in the NEAS and decreased towards oligotrophic waters of the SEAS. The strong coastal-offshore gradient in diatom distribution in both SEAS and NEAS ecosystem and little (significant) variability in coastal-offshore physical (chemical) parameters suggests that, the nutrient stoichiometry primarily defined the dominance of photosynthetic eukaryotes along the EAS (Fig. 7). The higher nutrient concentration in the mixed layer of the NEAS resulted in enhanced phytoplankton biomass in the surface layers, whereas the oligotrophic

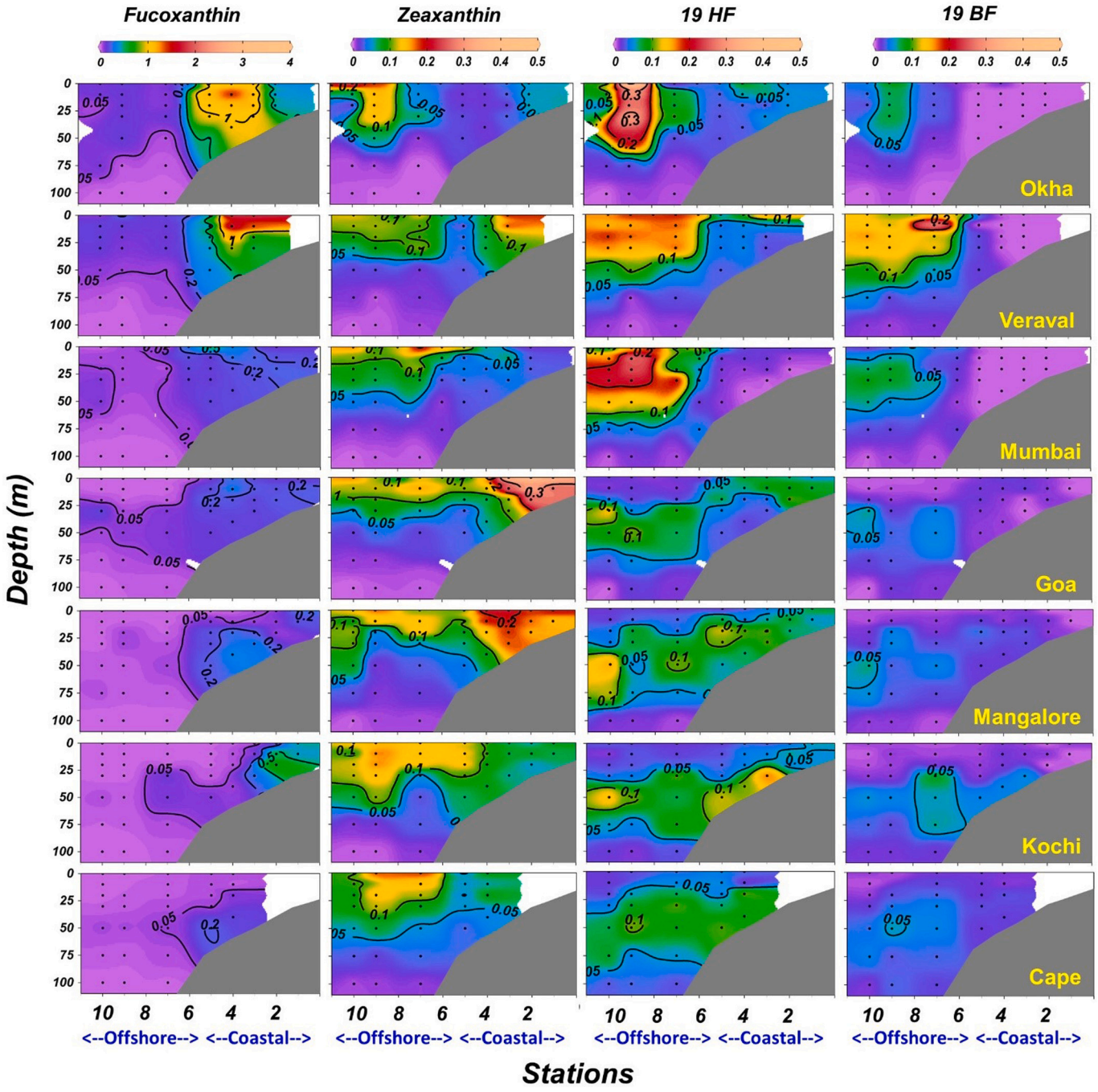

Fig. 4. (*continued*).

conditions in the SEAS mixed layer led to the formation of SCM close to the bottom of the MLD where relatively higher nutrients were recorded. Subsequently, the chlorophyll *a* was four times higher (1.54±1.31) in the NEAS than the oligotrophic SEAS (0.38±0.45 μg l^{-1}). Diatoms contributed up to 96% in the coastal stations of NEAS while its contributions decreased in the NEAS offshore stations (max. 40%). Diatoms continued to be the major group in the SEAS coastal (max. 55%) and offshore waters (max. 31%). Enhanced nutrient concentration associated with the macro-tidal environment of NEAS coastal waters significantly supported the proliferation of diatoms, particularly in the northernmost transects (Fig. 6g). The difference in nutrient concentration between SEAS and NEAS resulted in nearly 5–10 times lower diatom abundance in the former region than the latter. The statistical analysis revealed a significant role of silicate in controlling the micro phytoplankton in the coastal areas of NEAS. However, the Si/N ratio played a key role in the SEAS coastal waters (Fig. 7).

Though EAS is characterised by a considerable amount of silicate (SEAS: 2.0±0.4 μM; NEAS: 3.3±1.8 μM) in the mixed layer, the Si/N (SEAS: 1.6±0.9; NEAS: 1.6±0.8) and Si/P (SEAS: 8.7±5.0; NEAS: 6.4±1.6) ratios suggest that the relative abundance of silicate to other nutrients is less in the offshore waters, particularly in the NEAS. This may be the reason for a decrease in diatoms population in the nutrient-rich offshore regions of NEAS. This observation is supported by earlier studies that linked the decrease in diatom concentration in the offshore waters to its growth limitation due to the less availability of silicate in the MLD (Prakash et al., 2017; Sarma et al., 2019) while it provided a competitive advantage for prokaryotic groups.

In the EAS basin the pigments associated with nanoflagellates

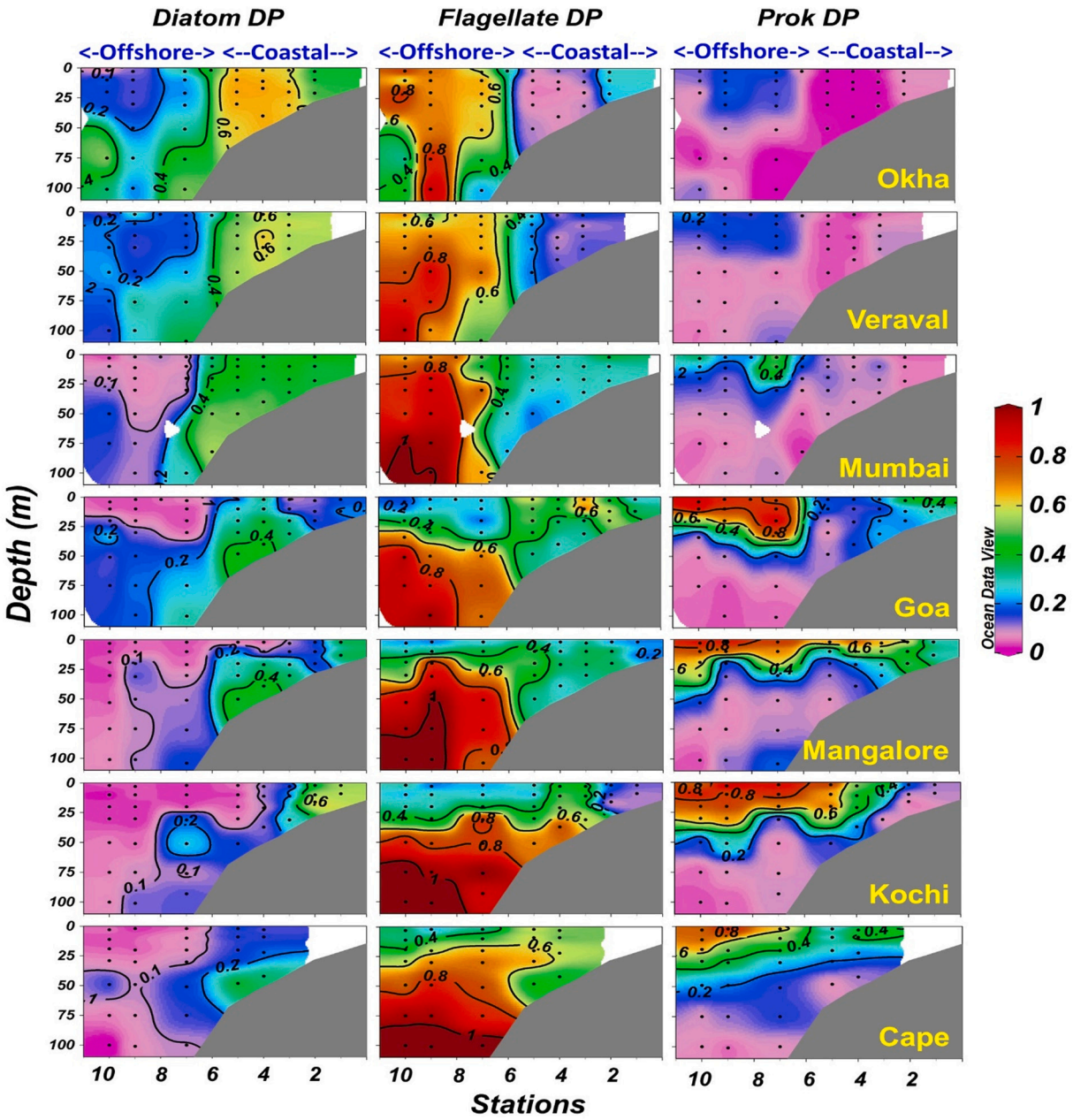

Fig. 5. Distribution of diagnostic pigment indices following Barlow et al. (2007) for (a) Diatoms (b) Flagellates (c) Prokaryotes along the EAS during WM 2018.

(19'hexanoyloxyfucoxanthin, 19'butanoyloxyfucoxanthin, Chl C3), showed clear vertical segregation in their distribution in both the SEAS and NEAS. These biomarker pigments for prymnesiophytes were more abundant in shallow layers of the mesotrophic NEAS water (Roy et al., 2015) and were confined to the SCM layer in the SEAS. The picoplankton community was represented by two major groups, *Prochlorococcus* and *Synechococcus,* which showed distinct spatial heterogeneity in their distributional pattern. The nutrient-rich offshore waters of the NEAS recorded a higher cyanobacterial population, particularly in the upper 50 m. Though the nitrate concentration was high (>1.5 μM) in the NEAS offshore waters (MLD), a low N/P ratio (4.9±2.3) supports the sustenance of a mix of eukaryotic and prokaryotic phytoplankton groups. The higher abundance of cyanobacteria in the NEAS region compared to the SEAS could be due to their preference to cool, high-saline, mesotrophic waters (Liu et al., 1998; Roy et al., 2015) over the oligotrophic conditions (Rajaneesh et al., 2020). The major factors found to affect the distribution of prochlorophytes are temperature and ambient nutrient conditions. The prochlorophytes recorded higher abundance (up to 84%) in the warmer (>27 °C), low saline (<33.5) SEAS offshore waters, decreased gradually towards the north and was completely absent in colder (<25 °C), high-saline (>36) waters. Shalapyonok et al. (2001) and Chndrasekhararao et al. (2018) reported *Prochlorococcus* proliferation in the warmer environment of AS. However, the present study recorded a statistically significant influence of salinity ($p<0.01$) in controlling the distribution of prochlorophytes in the AS. Earlier, Prasannakumar et al. (2004) and Narvekar et al. (2017) suggested an increase in chlorophyll in the SEAS waters associated with the intrusion of low saline waters from BoB during WM. This increase in chlorophyll *a* was attributed to the strengthening of West India Coastal Current that transported more chlorophyll as well as nutrient-rich waters from the Indo-Sri Lanka region toward the southern part of the EAS (Prasannakumar et al., 2004). A relatively higher nutrient supply (nitrate>0.5) associated with BoB waters was reported during early WM, December (Prasannakumar et al., 2004). Such an increase in nitrate levels was not

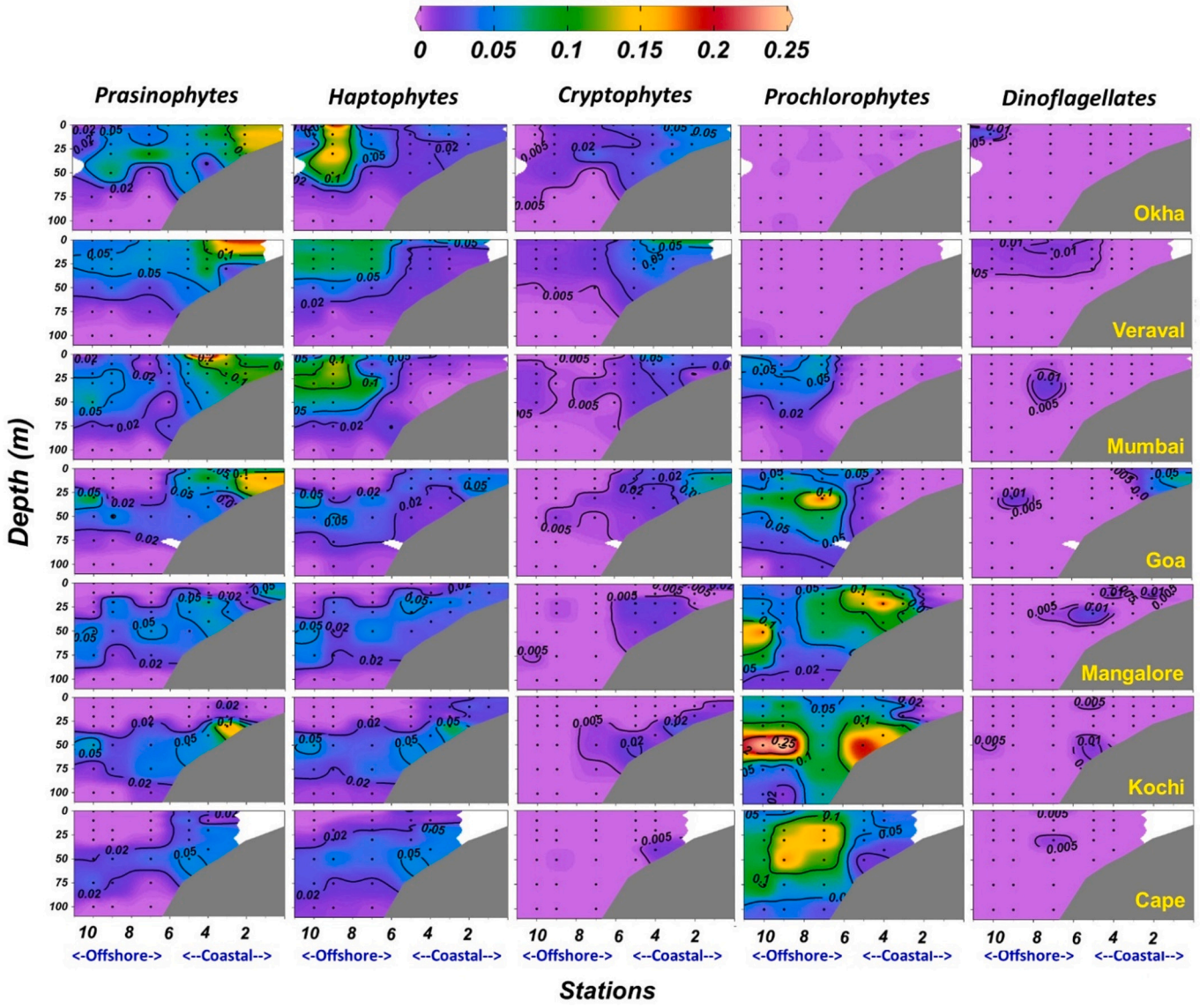

Fig. 6. The distribution of contribution of major phytoplankton groups (a) Prasinophytes (b) Haptophytes (c) Cryptophytes (d) Prochlorophytes (e) Dinoflagellates to TChl *a*, as estimated by interpretation of pigment HPLC data using the CHEMTAX program in μg l^{-1}. The distribution of contribution of major phytoplankton groups (f) Chlorophytes (g) Diatoms (h) Cyanobacteria to TChl *a*, as estimated by interpretation of pigment HPLC data using the CHEMTAX program in μg l^{-1}.

observed in the present study which was carried out during the peak WM (January); instead, higher levels of ammonium (>1 μM) were recorded (Fig. 3). Therefore, it is likely that the stratification induced by a warmer and low-saline environment of the SEAS significantly supported the proliferation of prochlorophytes which had a competitive advantage over other autotrophic groups in utilising inorganic nutrients like ammonium (Zubkov et al., 2002; Mouriño-Carballido et al., 2016).

In the present study, the zeaxanthin/DVChl *a* ratio was used as an index for the presence of prochlorophytes and was observed in trace or below detectable levels in the waters north of Mumbai. The absence of prochlorophytes in the NEAS waters could be due to water column instability associated with convective mixing that strongly regulates the picophytoplankton community composition (Roy and Anil, 2015; Bemal et al., 2018). However, the prochlorophytes thrived well in the relatively stable, stratified oligotrophic surface waters of the SEAS (Fig. 6d). This may be due to the competitive advantage of smaller *Prochlorococcus* cells over the other phytoplankton communities to efficient utiliation of nutrients even in oligotrophic waters (Mouriño-Carballido et al., 2016).

4.3. The relevance of phytoplankton community structure to food-web dynamics

The planktonic food-web structure primarily controls carbon cycling and the potential for a downward flux of carbon in the marine ecosystem (Garrison et al., 2000; Michaels and Silver, 1988). The present study shows the dominance of larger phytoplankton like diatoms in coastal waters of EAS, which suggests a herbivorous control on the food web (Legendre and Rassoulzadegan, 1995). The micro phytoplankton can sink directly and contribute more to the sinking flux of organic matter compared to the smaller fractions due to the longer food chain they are involved with. The picoplankton which formed a major group in offshore waters was earlier assumed to be a negligible component of the zooplankton diet (Kiørboe, 2011) and hence thought to have little contribution to sinking material. Ever since their link with meso-zooplankton through micro grazing was established, they have risen in importance with respect to carbon sink and food web dynamics (Roman et al., 1995; Motwani and Gorokhova, 2013) especially in regions with severe nitrogen limitation (Sohm et al., 2011). A recent study conducted

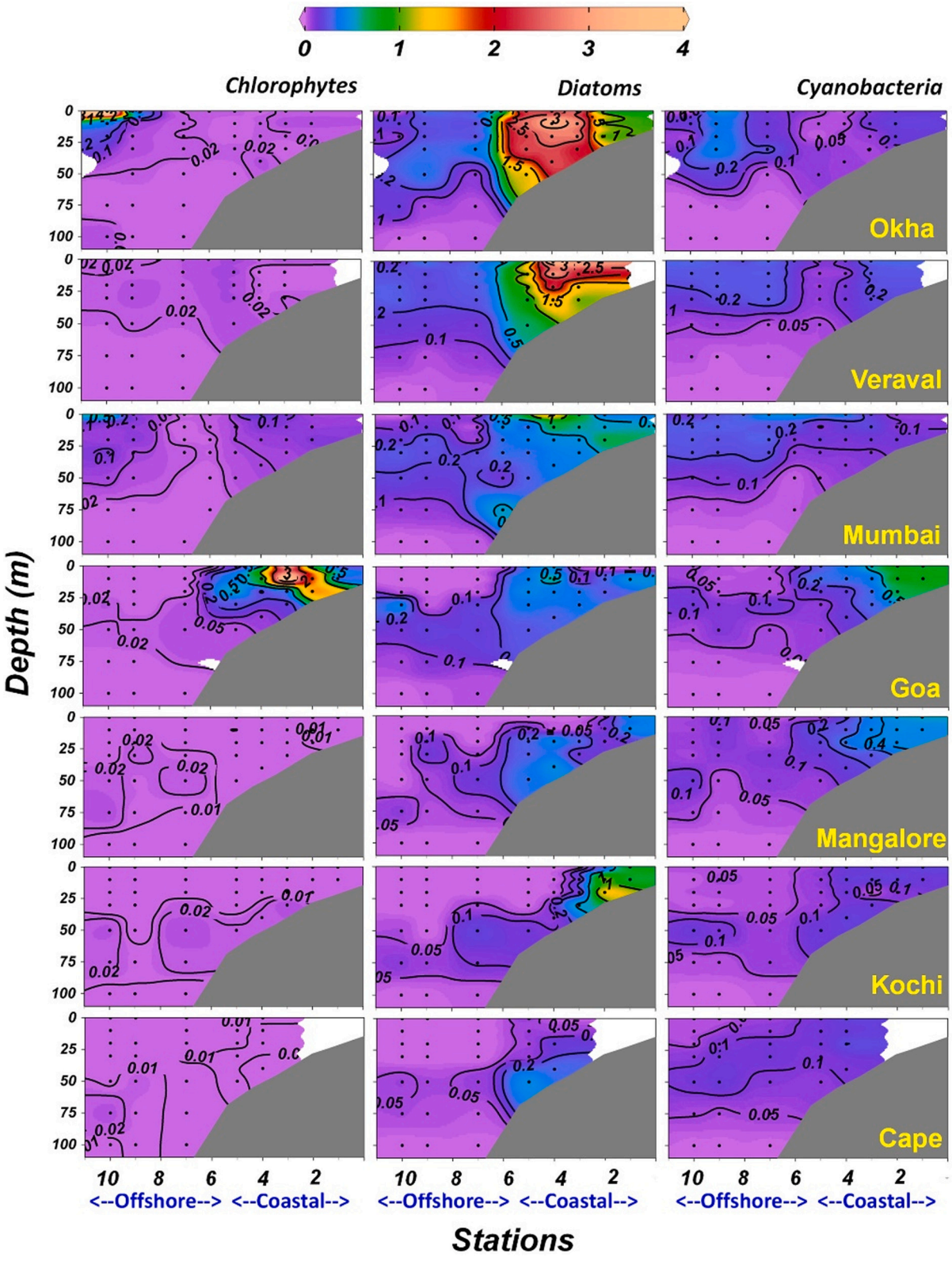

Fig. 6. (*continued*).

during WM in the NEAS reported significantly higher carbon contribution by picoplankton (*Synechococcus*) (1.37 μg C l^{-1}) (Bemal et al., 2018). The large proportion of pico-nano plankton in the offshore waters indicates a transition of the ecosystem to a mixotrophic condition, where the micro fraction of phytoplankton still has a significant contribution. Moreover, the coastal waters are dominated with large phytoplankton like diatoms, more prominently in the NEAS, which are suggested to favour herbivorous food-web. On the other hand, a long-standing hypothesis attributes carnivorous fishery in the NEAS to longer food chains (Madhupratap et al., 2001; Shankar et al., 2019). The reason for this discrepancy needs further investigation, giving due consideration to the seasonal dynamics at different levels of the food-web.

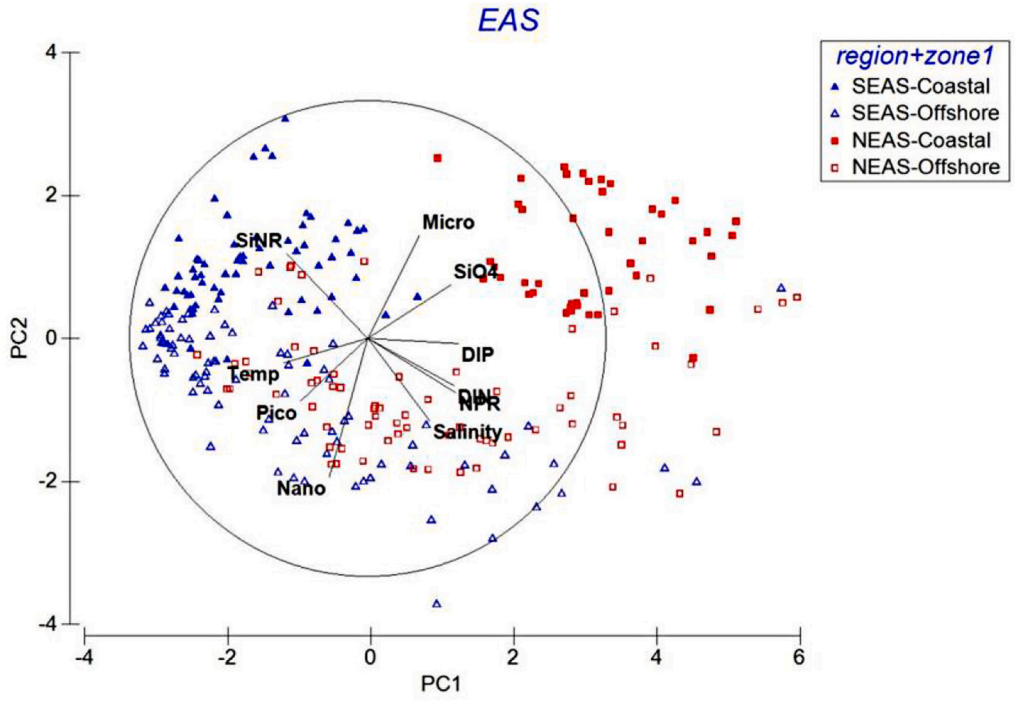

Variable	PC1	PC2
Temp	**-0.353**	-0.104
Salinity	0.261	**-0.347**
DIP	0.382	-0.022
SiO4	0.35	0.226
NPR	**0.37**	-0.228
SiNR	**-0.341**	0.357
Micro	0.216	**0.433**
Nano	-0.161	**-0.583**
Pico	-0.284	-0.265
DIN	**0.364**	-0.2

PC	Eigenvalues	%Variation	Cum.%Variation
1	5.69	56.9	56.9
2	1.51	15.1	72
3	0.957	9.6	81.6
4	0.573	5.7	87.3
5	0.446	4.5	91.8

Fig. 7. Results of principal component analysis showing the relation of phytoplankton functional groups to environmental parameters.

5. Conclusion

The present study detailed the distribution of phytoplankton community structure (using HPLC- based pigment analysis) along the eastern Arabian Sea (EAS). The NEAS was characterised by the cold, high saline, nutrient-rich environment while warm, low saline, oligotrophic conditions prevailed over the SEAS. This difference in physico-chemical settings was found to be responsible for the variability in phytoplankton communities in the two regions. Diatoms were the dominant group in the coastal regions of the entire EAS basin with a maximum abundance observed in the NEAS waters and were found to be chiefly controlled by nutrient availability. The dominance of cyanobacterial and prymnesiophyte population in the NEAS offshore and prochlorophytes in the SEAS offshore were predominantly influenced by both physical and chemical conditions during WM. The warm oligotrophic environment led to a stratified condition with well-defined SCM in the SEAS, which was dominated by picophytoplankton abundance. The large proportion of pico-nano plankton in the offshore of EAS suggests a transition of the ecosystem to a mixotrophic condition where micro-fraction of phytoplankton continued to contribute to the total phytoplankton biomass. The dominance of large phytoplankton like diatoms indicates a herbivorous control in the food chain in coastal waters of EAS. Its implication on food web dynamics should be studied further, considering annual cyclicity in phytoplankton community structure.

Declaration of Competing Interest

None.

Acknowledgements

Authors would like to thank Dr.M. Sudhakar (former Director), Centre for Marine Living Resources and Ecology (CMLRE), Kochi for providing facilities to carry out the study. We are grateful to the scientific team of the cruises of FORV *Sagar Sampada* for their help in the

sampling. This study was carried out as part of the *Marine Ecosystem Dynamics of eastern Arabian Sea* (MEDAS) programme funded by the Ministry of Earth Sciences, Govt. of India, New Delhi, and implemented by CMLRE, Kochi. We are thankful to the Captain, Chief Engineer, and the entire crew of FORV *Sagar Sampada*. The authors wish to acknowledge the help rendered by Dr(s). Abdul Jaleel K. U. and Usha V. Parameswaran in the statistical analysis and Dr. A.V. Chndrasekhararao in the fieldwork. This is the CMLRE contribution No.128.

References

Ahmed, A., Kurian, S., Gauns, M., Chndrasekhararao, A.V., Mulla, A., Naik, B., Naik, H., Naqvi, S.W.A., 2016. Spatial variability in phytoplankton community structure along the eastern Arabian Sea during the onset of south-west monsoon. Cont. Shelf Res. 119, 30–39.

Baliarsingh, S.K., Aneesh, A.L., Sudheesh, V., Alakes, S., Sourav, D., Vijayan, A.K., 2018. Response of phytoplankton community and size classes to green Noctiluca bloom in the northern Arabian Sea. Mar. Poll. Bull. 129, 222–230.

Banse, K., 1987. Seasonality of phytoplankton chlorophyll in the central and northern Arabian Sea. Deep-Sea Res. I. 34, 713–723.

Banse, K., English, D.C., 1993. Revision of satellite-based phytoplankton pigment data from the Arabian Sea during the northeast monsoon. Mar.Res.(Pakistan) 2, 83–103.

Barlow, R.G., Mantoura, R.F.C., Cummings, D.G., 1999. Monsoonal influence on the distribution of phytoplankton pigments in the Arabian Sea. Deep-Sea Res. II. 46, 677–699.

Barlow, R.G., Aiken, J., Holligan, P.M., Cummings, D.G., Maritorena, S., Hooker, S., 2002. Phytoplankton pigment and absorption characteristics along meridional transects in the Atlantic Ocean. Deep-Sea Res. I. 47, 637–660.

Barlow, R., Stuart, V., Lutz, V., Sessions, H., Sathyendranath, S., Platt, T., Kyewalyanga, M., Clementson, L., Fukasawa, M., Watanabe, S., Devred, E., 2007. Seasonal pigment patterns of surface phytoplankton in the subtropical southern hemisphere. Deep-Sea Res. I. 54, 1687–1703.

Bemal, S., Anil, A.C., Shankar, D., Remya, R., Roy, R., 2018. Picophytoplankton variability: influence of winter convective mixing and advection in the northeastern Arabian Sea. J. Mar. Syst. 180, 37–48.

Bhattathiri, P.M.A., Pant, A., Sawant, S., Gauns, M., Matondkar, S.G.P., Mohanraju, R., 1996. Phytoplankton production and chlorophyll distribution in the eastern and central Arabian Sea. Curr. Sci. 71 (11), 857–862.

Bidigare, R.G., Charles, C.T., 2002. HPLC phytoplankton pigments: sampling, laboratory methods and quality assurance procedures. In: Fargion, G.S., Muellier, J.L. (Eds.), Protocols For Satellite Ocean Colour Validation Revision 2. NASA, Goddard Space Flight Centre, Greenbelt, MD, pp. 154–160.

Bouman, H.A., Platt, T., Sathyendranath, S., Li, W.K.W., Stuart, V., Fuentes-Yaco, C., Maass, H., Horne, E.P.W., Ulloa, O., Lutz, V., Kyewalyanga, M., 2003. Temperature as indicator of optical properties and community structure of marine phytoplankton: implications for remote sensing. Mar. Ecol. Prog. Ser. 258, 19–30.

Bouman, H.A., Platt, T., Sathyendranath, S., Stuart, V., 2005. Dependence of light-saturated photosynthesis on temperature and community structure. Deep-Sea Res. I. 52, 1284–1299.

Brown, S.L., Landry, M.R., Christensen, S., Garrison, D., Gowing, M.M., Bidigare, R.R., Campbell, L., 2002. Microbial community dynamics and taxon-specific phytoplankton production in the Arabian Sea during the 1995 monsoon seasons. Deep-Sea Res. II. 49, 2345–2376.

Chacko, P.I., 1942. An unusual incidence of mortality of marine fauna. Curr. Sci. 11, 406–407.

Charpy, L., Blanchot, J., 1996. Photosynthetic picoplankton in French Polynesian atoll lagoons: Estimation of taxa contribution to biomass and production by flow cytometry. Mar. Ecol. Prog. Ser. 162, 57–70.

Chisholm, S.W., 1992. Phytoplankton size. In: Falkowski, P.G., Woodhead, A.D. (Eds.), Primary Productivity and Biogeochemical Cycles in the Sea. Plenum Press, New York, pp. 213–237.

Chndrasekhararao, A.V., Kurian, S., Vidya, P.J., Gauns, M., Shenoy, D.M., Mulla, A., Naik, H., Reddy, T.V., Naqvi, S.W.A., 2018. Phytoplankton response to the contrasting physical regimes in the eastern Arabian Sea during north east monsoon. J. Mar. Syst. 182, 56–66.

Devassy, V.P., Bhattathiri, P.M.A., Qasim, S.Z., 1978. Trichodesmium phenomenon. Indian J. Mar. Sci. 7, 168–186.

Devassy, V.P., Bhattathiri, P.M., Qasim, S.Z., 1979. Succession of organisms following Trichodesmium phenomenon. Indian J. Mar. Sci. 8, 89–93.

Devassy, V.P., Goes, J.I., 1988. Phytoplankton community structure and succession in a tropical estuarine complex (Central west coast of India). Estuar. Coast. Shelf Sci. 27, 671–685.

García-Robledo, E., Corzo, A., Papaspyrou, S., 2014. A fast and direct spectrophotometric method for the sequential determination of nitrate and nitrite at low concentrations in small volumes. Mar. Chem. 162, 30–36.

Garrison, D.G., Gowing, M.M., Hughes, M.P., Campbell, L., Caron, D.A., Dennett, M.R., Shalapyonok, A., Olson, R.J., Landry, M.R., Brown, S.L., Liu, H.-B., Azam, F., Steward, G.F., Ducklow, H.W., Smith, D.C., 2000. Microbial food web structure in the Arabian Sea: A US JGOFS study. Deep-Sea Res. II. 47, 1387–1422.

Gibb, S.W., Cummings, D.G., Irigoien, X., Barlow, R.G., Fauzi, R., Mantoura, R.F.C., 2001. Phytoplankton pigment chemotaxonomy of the northeastern Atlantic. Deep-Sea Res. II. 48, 795–823.

Goericke, R., 2002. Top-down control of phytoplankton biomass and community structure in the monsoonal Arabian Sea. Limnol. Oceanogr. 47, 1307–1323.

Goes, J.I., Gomes, H., Kumar, A., Gouveia, A.D., Devassy, V.P., Parulekar, A.H., Rao, L.V. G., 1992. Satellite and ship studies of phytoplankton along the west coast of India. In: Desai, B.N. (Ed.), Oceanography of the Indian Ocean, pp. 67–80. Ed. by.

Gomes, H.R., Goes, J.I., Matondkar, S.G.P., Parab, S.G., Al-Azri, A.R.N., Thoppil, P.G., 2008. Blooms of Noctiluca miliaris in the Arabian Sea—An in situ and satellite study. Deep-Sea Res. I. 55, 751–765.

Grasshoff, K., Ehrhardt, M., Kremling, K. (Eds.), 1999. Methods of Sea Water Analysis, 3rd ed. VCH, Wainheins, Germany.

Gupta, G.V.M., Sudheesh, V., Sudharma, K.V., Saravanane, N., Dhanya, V., Dhanya, K.R., Lakshmi, G., Sudhakar, M., Naqvi, S.W.A., 2016. Evolution to decay of upwelling and associated biogeochemistry over the southeastern Arabian Sea shelf. J. Geophys. Res. Biogeosci. 121 https://doi.org/10.1002/2015JG003163.

Jeffrey, S.W., Vesk, M., 1997. Introduction to marine phytoplankton and their pigment signatures. In: Jeffrey, S.W., Mantoura, R.F.C., Wright, S.W. (Eds.), Phytoplankton Pigments in Oceanography: Guidelines to Modern Methods. UNESCO Publ, Paris, pp. 37–84.

Jeffrey, S.W., Wright, S.W., 1997. Qualitative and quantitative HPLC analysis of SCOR reference algal cultures. In: Jeffrey, S.W., Mantoura, R.F.C., Wright, S.W. (Eds.), Phytoplankton Pigments in Oceanography: Guidelines to Modern Methods. UNESCO, Paris, pp. 343–360. Eds.

Jeffrey, S.W., Mantoura, R.F.C., Wright, S.W. (Eds.), 1997. Phytoplankton Pigments in Oceanography. UNESCO Publishing, Paris, p. 661.

Jochem, F.J., 2003. Photo- and heterotrophic pico- and nanoplankton in the Mis- sissippi River plume: Distribution and grazing activity. J. Plankton Res. 25, 1201–1214.

John, C.C., Menon, M.A.S., 1942. Food and feeding habits of the oil sardine and mackerel. Curr. Sci. 11, 243–244.

Kiørboe, T., 2011. How zooplankton feed: mechanisms, traits and trade-offs. Biol. Rev. 86, 311–339.

Krishnankutty, S., Joseph, C.A., Vincent, P.D., Jabir, T., Vishnu, P.S., Saramma, A.V., Hatha, A.A.M., 2019. Hydrographic, seasonal diversity, distribution and abundance of phytoplankton in coastal waters off Cochin - south-eastern Arabian Sea. Indian J. Mar. Sci. 48 (03), 319–326.

Latasa, M., Bidigare, R., 1998. A comparison of phytoplankton populations of the Arabian Sea during the Spring Intermonsoon and Southwest Monsoon of 1995 as described by HPLC-analyzed pigments. Deep-Sea Res. II. 45, 2133–2170.

Legendre, L., Demers, S., 1984. Towards dynamic biological oceanography and limnology. Can. J. Fish. Aquat. Sci. 41, 2–19.

Legendre, L., Rassoulzadegan, F., 1995. Plankton and nutrient dynamics in coastal waters. Ophelia. 41, 153–172.

Liu, H., Campbell, L., Landry, M.R., Nolla, H.A., Brown, S.L., Constantinou, J., 1998. *Prochlorococcus* and *Synechococcus* growth rates and contributions to production in the Arabian Sea during the 1995 Southwest and Northeast Monsoons. Deep-Sea Res. II. 45, 2327–2352.

Lotliker, A.A., Baliarsingh, S.K., Trainer, V.L., Wells, M.L., Wilson, C., Udaya Bhaskar, T. V.S., Samanta, A., Shahimol, S.R., 2018. Characterization of oceanic Noctiluca blooms not associated with hypoxia in the Northeastern Arabian Sea. Harmful Algae. 74, 46–57.

Mackey, M.D., Mackey, D.J., Higgins, H.W., Wright, S.W., 1996. CHEMTA—a program for estimating class abundances from chemical markers: application to HPLC measurements of phytoplankton. Mar. Ecol. Prog. Ser. 144, 265–283.

Madhupratap, M., Prasanna Kumar, S., Bhattathiri, P.M.A., Dileep Kumar, M., Raghukumar, S., Nair, K.K.C., Ramaiah, N., 1996. Mechanism of the biological response to winter cooling in the northeastern Arabian Sea. Nature. 384, 549–552.

Madhupratap, M., Nair, K.N.V., Gopalakrishnan, T.C., Haridas, P., Nair, K.K.C., Venugopal, P., Gauns, M., 2001. Arabian Sea Oceanography and fisheries of the west coast of India. Curr. Sci. 81, 355–361.

Matondkar, S.G.P., Parab, S., Dwivedi, R.M., 2006. Seasonality in sub-surface chlorophyll maxima in the Arabian Sea: detection by IRS-P4/OCM and implication of it to primary productivity. In: Proceedings of SPIE - The International Society for Optical Engineering. 6406, art. no. 64060X.

Michaels, A.F., Silver, M.W., 1988. Primary production, sinking fluxes and the microbial food web. Deep-Sea Res. 35, 473–490.

Minu, P., Shaju, S.S., Ashraf, P.M., Meenakumari, B., 2014. Phytoplankton community characteristics in the coastal waters of the southeastern Arabian Sea. Acta Oceanol. Sin. 33 (12), 170–179.

Mitbavkar, S., Rajaneesh, K., Anil, A., Sundar, D., 2012. Picophytoplankton community in a tropical estuary: Detection of Prochlorococcus-like populations. Estuar. Coast. Shelf Sci. 107, 159–164.

Motwani, N.H., Gorokhova, E., 2013. Mesozooplankton grazing on picocyanobacteria in the Baltic Sea as inferred from molecular diet analysis. PLoS One. 8 (11), e79230.

Mouriño-Carballido, B., Hojas, E., Cermeño, P., Chouciño, P., Fernández-Castro, B., Latasa, M., Marañón, E., Morán, X.A.F., Vidal, M., 2016. Nutrient supply controls picoplankton community structure during three contrasting seasons in the northwestern Mediterranean Sea. Mar. Ecol. Prog. Ser. 543, 1–19.

Narvekar, J., D'Mello, J.R., Prasanna Kumar, S., Banerjee, P., Sharma, V., Shenai-Tirodkar, P., 2017. Winter-time variability of the eastern Arabian Sea: A comparison between 2003 and 2013. Geophys. Res. Lett. 44 https://doi.org/10.1002/2017GL072965.

Padmakumar, K.B., Smitha, B.R., Thomas, L.C., Fanimol, C.L., SreeRenjimma, G., Menon, N.R., Sanjeevan, V.N., 2010. Blooms of *Trichodesmium erythraeum* in the South Eastern Arabian Sea during the onset of 2009 Summer Monsoon. Ocean Sci. J. 45 (3), 151–157.

Parab, S.G., Matondkar, S.G.P., Gomes, H.R., Gomes, J.I., 2006. Monsoon driven changes in phytoplankton populations in the eastern Arabian Sea as revealed by microscopy and HPLC pigment analysis. Cont. Shelf Res. 26 (20), 2538–2558.

Prakash, S., Roy, R., Lotliker, A., 2017. Revisiting the *Noctiluca scintillans* paradox in northern Arabian Sea. Curr. Sci. 113, 1429–1434.

Prasannakumar, S., Narvekar, J., Kumar, A., Shaji, C., Anand, P., Sabu, P., Rijomon, G., Josia, J., Jayaraj, K.A., Radhika, A., Nair, K.K.C., 2004. Intrusion of the Bay of Bengal water into the Arabian Sea during winter monsoon and associated chemical and biological response. Geophys. Res. Lett. 31, L15304 https://doi.org/10.1029/2004GL020247.

Qasim, S.Z., 1977. Biological productivity of the Indian Ocean. Indian J. Mar. Sci. 6, 122–137.

Radhakrishna, K., Devassy, V.P., Bhattathiri, P.M.A., Bhargava, R.M.S., 1978. Primary productivity in the North-Eastern Arabian Sea. Ind. J. Mar. Sci. 7, 137–139.

Rai, S.V., Rajashekhar, M., 2014. Seasonal assessment of hydrographic variables and phytoplankton community in the Arabian Sea waters of Kerala, southwest coast of India. Braz. J. Oceanogr. 62 (4), 279–293.

Rajaneesh, K.M., Naik, R.K., Roy, R., D'Costa, P.M., 2020. Cyanobacteria in tropical and subtropical marine environments: bloom formation and ecological role (Eds.). In: Singh, P.K., Kumar, A., Singh, V.K., Shrivastava, A.K. (Eds.), Advances in Cyanobacterial Biology, pp. 35–46. https://doi.org/10.1016/B978-0-12-819311-2.00003-6.

Redfield, A.C., 1958. The biological control of chemical factors in the environment. Am. Sci. 46, 205–221.

Roman, M.R., Dam, H.G., Gauzens, A.L., Urban-Rich, J., Foley, D.G., Dickey, T.D., 1995. Zooplankton variability on the equator at 140°W during the JGOFS EqPac study. Deep-Sea Res. II. 42 (2-3), 673–693.

Roy, R., Anil, A.C., 2015. Complex interplay of physical forcing and *Prochlorococcus* population in ocean. Progr. Oceanogr. 137, 250–260.

Roy, R., Chitari, E., Kulkarni, V., 2015. CHEMTAX-derived phytoplankton community structure associated with temperature fronts in the northeastern Arabian Sea. J. Mar. Syst. 144, 81–91.

Roy, R., Prathihary, A.K., Mangesh, G., Naqvi, S.W.A., 2006. Spatial variation of phytoplankton pigments along the southwest coast of India. Estuar. Coast. Shelf Sci. 69, 189–195.

Roy, R., 2010. Short-term variability in halocarbons in relation to phytoplankton pigments in coastal waters of the central eastern Arabian Sea. Estuar. Coast. Shelf. S. 88 (3), 311–321.

Sarma, V.V.S.S., Desai, D.V., Patil, J.S., Khandeparker, L., Aparna, S.G., Shankar, D., D'Souza, S., Dalabehera, H.B., Mukherjee, J., Sudharani, P., Anil, A.C., 2018. Ecosystem response in temperature fronts in the northeastern Arabian Sea. Prog. Oceanogr. 165, 317–331.

Sarma, V.V.S.S., Patil, J.S., Shankar, D., Anil, A.C., 2019. Shallow convective mixing promotes massive *Noctiluca scintillans* bloom in the northeastern Arabian Sea. Mar. Poll. Bull. 138, 428–436.

Sawant, S., Madhupratap, M., 1996. Seasonality and composition of phytoplankton in the Arabian Sea. Curr. Sci. 17, 869–873.

Schlüter, L., Møhlenberg, F., Havskum, H., Larsen, S., 2000. The use of phytoplankton pigments for identifying and quantifying phytoplankton groups in coastal areas: testing the influence of light and nutrients on pigment/chlorophyll *a* ratios. Mar. Ecol. Prog. Ser. 192, 49–63.

Shalapyonok, A., Olson, R., Shalapyonok, L., 2001. Arabian Sea phytoplankton during Southwest and Northeast Monsoons 1995: Composition, size structure and biomass from individual cell properties measured by flow cytometry. Deep-Sea Res. II. 48, 1231–1261.

Shankar, D., Remya, R., Anil, A.C., Vijith, V., 2019. Role of physical process in determining the nature of fisheries in the eastern Arabian Sea. Prog. Oceanogr. 172, 124–158.

Sohm, J.A., Webb, E.A., Capone, D.G., 2011. Emerging patterns of marine nitrogen fixation. Nat. Rev. Microbiol. 9 (7), 499–508.

Subrahmanyan, R., Sarma, A.H.V., 1961. Studies on the phytoplankton of the west coast of India. Part III, Seasonal variation of the phytoplankton and environmental factors. Ind. J. fish. 7, 307–336.

Subrahmanyan, R., Sarma, A.H.V., 1967. Studies on the phytoplankton of the west coast of India. Part IV, magnitude of the standing crop for 1955–1962, with observations on nanoplankton and its significance to fisheries. J. Mar. Biol. Assoc. India. 7, 406–419.

Thomas, L.C., Padmakumar, K.B., Smitha, B.R., Asha Devi, C.R., BijoyNandan, S., Sanjeevan, V.N., 2013. Spatio-temporal variation of microphytoplankton in the upwelling system of the south-eastern Arabian Sea during the summer monsoon of 2009. Oceanologia. 55 (1), 185–204.

Trees, C.C., Clark, D.K., Bidigare, R.R., Ondrusek, M.E., Mueller, J.L., 2000. Accessory pigments versus chlorophyll *a* concentration within the euphotic zone: A ubiquitous relationship. Limnol. Oceanogr. 45 (5), 1130–1143.

Uitz, J., Claustre, H., Morel, A., Hooker, S.B., 2006. Vertical distribution of phytoplankton communities in open ocean: An assessment based on surface chlorophyll. J. Geophys. Res. 111, C08005 https://doi.org/10.1029/2005JC003207.

Van Heukelem, L., 2002. HPLC phytoplankton pigments: sampling, laboratory methods, and quality assurance procedures. In: Mueller, J., Fargion, G. (Eds.), Ocean Optics Protocols for Satellite Ocean Color Sensor, Revision 3, Volume 2, Chapter16, NASA Technical Memorandum 2002–2004, vol. 2, pp. 258–268.

Vaulot, D., Partensky, F., Neveux, J., Mantoura, R.F.C., Llewellyn, C.A., 1990. Winter presence of prochlorophytes in surface waters of the northwestern Mediterranean Sea. Limnol. Oceanogr. 35, 1156–1164.

Vidussi, F., Clustre, H., Manca, B.B., Luchetta, A., Marty, J.C., 2001. Phytoplankton pigment distribution in relation to upper thermocline circulation in the eastern Mediterranean Sea during winter. J. Geophys. Res. 106, 19939–19956.

Warwick, R., Clarke, K., 2006. PRIMER 6. PRIMER-E Ltd, Plymouth, p. 615.

Wiggert, J.D., Murtugudde, R.G., McClain, C.R., 2002. Processes controlling interannual variations in wintertime (Northeast Monsoon) primary productivity in the central Arabian Sea. Deep-Sea Res. II. 49, 2319–2343.

Wiggert, J.D., Hood, R.R., Banse, K., Knindle, J.C., 2005. Monsoon-driven biogeochemical processes in the Arabian Sea. Prog. Oceanogr. 65, 176–213.

Wright, S.W., Jeffrey, S.W., Mantoura, R.F.C., Llewellyn, C.A., Bjørnland, T., Repeta, D., Welschmeyer, N., 1991. Improved HPLC method for the analysis of chlorophylls and carotenoids from marine phytoplankton. Mar. Ecol. Prog. Ser. 77, 183–196.

Wright, S.W., Ishikawa, A., Marchant, H.J., Davidson, A.T., van den Enden, R.L., Nash, G. V., 2009. Composition and significance of picophytoplankton in Antarctic waters. Pol. Biol. 32, 797–808.

Wright, S.W., van den Enden, R.L., Pearce, I., Davidson, A.T., Scott, F.J., Westwood, K.J., 2010. Phytoplankton community structure and stocks in the Southern Ocean (30–80 E) determined by CHEMTAX analysis of HPLC pigment signatures. Deep-Sea Res. II. 57, 758–778.

Zubkov, M.V., Fuchs, B.M., Tarran, G.A., Burkill, P.H., Amann, R., 2002. High rate of uptake of organic nitrogen compounds by Prochlorococcus Cyanobacteria as a key to their dominance in oligotrophic oceanic waters. Appl. Environ. Microbiol. 69 (2), 1299–1304.